E. Babaev, J. Carlström, M. Silaev, and J.M. Speight

4 Type-1.5 superconductivity

4.1 Introduction

In the simplest case, a superconductor is described by a single complex order parameter field. The corresponding field theory has two fundamental length scales, the magnetic field penetration depth λ and the characteristic length scale associated with the order parameter, the coherence length ξ. Their ratio κ determines the response of a superconductor to an external field, sorting them into two categories as follows: type-1 when $\kappa < 1/\sqrt{2}$ and type-2 when $\kappa > 1/\sqrt{2}$. This theory has a critical point at $\kappa = 1/\sqrt{2}$ (the Bogomol'nyi point). However, in general, a superconducting state breaks multiple symmetries and is described by a multicomponent theory, characterized by several different coherence lengths ξ_i. As a result, there can appear a state where $\xi_1 \leq \xi_2 \ldots < \sqrt{2}\lambda < \xi_n \leq \ldots \xi_m$, that has no counterpart in the single-component case. This state was recently termed "type-1.5" superconductivity. Breakdown of the type-1/type-2 dichotomy is rather generic near a phase transition between superconducting states with different symmetries. Examples include the transitions between $U(1)$ and $U(1) \times U(1)$ states or between $U(1)$ and $U(1) \times Z_2$ states. The latter case is realized, for example, in systems that feature transition between s_{++}/s_{+-} and $s + is$ states, because the $s + is$ state spontaneously breaks time-reversal symmetry. Moreover, certain multiband superconductors that break only a single symmetry are nonetheless described by **multiband Ginzburg–Landau theory**. The extra fundamental length scales have many physical consequences. In particular, in these regimes vortices can attract one another at long range but repel at shorter ranges. Such a system can form vortex clusters in low magnetic fields. **Vortex clustering** in the type-1.5 regime gives rise to many physical effects, ranging from macroscopic phase separation in domains of different broken symmetries, to unusual phase transitions and transport properties.

Type-1 superconductors expel weak magnetic fields, while strong fields give rise to macroscopic phase separation in the form of domains of Meissner and normal states [1, 2]. The response of type-2 superconductors is the following [3]: below some critical value H_{c1}, the field is expelled. Above this value a superconductor forms a lattice or a liquid of vortices which carry magnetic flux through the system. Only at a higher second critical value, H_{c2} is superconductivity destroyed. These different responses are the consequences of the form of the vortex interaction in these systems,

E. Babaev, M. Silaev, Department of Theoretical Physics and Center for Quantum Materials, The Royal Institute of Technology, Stockholm SE-10691, Sweden
J. Carlström, Department of Physics, University of Massachusetts, Amherst MA 01003, USA
J.M. Speight, School of Mathematics, University of Leeds, Leeds LS2 9JT, UK

DOI 10.1515/9783110456806-005,

the energy cost of a boundary between superconducting and normal states and the thermodynamic stability of vortex excitations. In a type-2 superconductor the energy cost of a boundary between the normal and the superconducting state is negative, while the interaction between vortices is repulsive [3]. This leads to the formation of stable vortex lattices and liquids. In type-1 superconductors the situation is the opposite; the vortex interaction is attractive (thus making them unstable against collapse into one large "giant" vortex), while the boundary energy between normal and superconducting states is positive. The 'ordinary' Ginzburg–Landau model has a critical regime where vortices do not interact [4, 5]. The critical value of κ in the most common GL (Ginzburg–Landau) model parameterization corresponds to $\kappa = 1/\sqrt{2}$ (often the factor $\sqrt{2}$ is absorbed into the definition of coherence length in which case the critical coupling is $\kappa = 1$). The noninteracting regime, which is frequently called the "Bogomol'nyi limit" is a property of the Ginzburg–Landau model where, at $\kappa = 1/\sqrt{2}$, the core-core attractive interaction between vortices exactly cancels the current-current repulsive interaction [4, 5]. However, in a realistic condensed matter system, even in the limit $\kappa = 1/\sqrt{2}$, there will always be leftover intervortex interactions, appearing beyond the GL field-theoretic description, from underlying microscopic physics. The form of that interaction potential is determined not by the fundamental length scales of the GL theory but by nonuniversal microscopic physics, and it can indeed be nonmonotonic [6]. These microscopic corrections are extremely small. However, they are relevant in a very narrow window of parameters near $\kappa \approx 1/\sqrt{2}$, where intervortex forces in GL theory are also very small. By contrast in multicomponent theories type-1 and type-2 regimes are not in general separated by a Bogomol'nyi point.

The Ginzburg–Landau free energy functional for a multicomponent superconductor has the form

$$F = \frac{1}{2}\sum_i (D\psi_i)(D\psi_i)^* + V(\psi_i) + \frac{1}{2}(\nabla \times \mathbf{A})^2 \,, \tag{4.1}$$

where ψ_i are complex superconducting components, $D = \nabla + ie\mathbf{A}$, and $\psi_i = |\psi_i| e^{i\theta_i}$, $a = 1, 2$, and $V(\psi_i)$ stands for effective potential. We consider a general form of the potential terms but the simplest gradient terms. In general however Equation (4.1) can be augmented with mixed (with respect to the components ψ_i) gradient terms, e.g., $\mathrm{Re}[D_{\alpha=x,y,z}\psi_i D_{\beta=x,y,z}\psi_j]$. (For more details on the effects of these terms see [7].)

The multiple superconducting components can have various origins. First of all they can arise in *(i) superconducting states which break multiple symmetries*. Such systems are described by several order parameters in the sense of Landau's theory of phase transitions, and have different coherence lengths associated with them. Multiple broken symmetries are present even in the simplest generalization of the s-wave superconducting states: the $s+is$ superconducting state [8, 9], which breaks $U(1)\times Z_2$ symmetry [10]. Likewise, multiple broken symmetries are present in non-s-wave superconductors. Another example is mixtures of independently conserved condensates such as models for the theoretically discussed superconductivity in metallic hydrogen and hydrogen-rich alloys [11, 12]. There, ψ_i represents electronic and protonic Cooper

pairs or deuteronic condensates. A similar situation was discussed in certain models of nuclear superconductors in the interior of neutron stars, where ψ_i represent protonic and Σ^- hyperonic condensates [13, 14].

Another class of multicomponent superconductors is *(ii) systems which are described by multicomponent Ginzburg–Landau field theories that do not originate in multiple broken symmetries*. The most common examples are multiband superconductors [15–17]. In this case, ψ_i represent superconducting components belonging to different bands. Since a priori there are no symmetry constraints preventing interband Cooper pair tunneling the theory contains generic terms which describe intercomponent Josephson coupling, $\frac{\eta}{2}(\psi_i\psi_j^* + \psi_i\psi_j^*)$. These terms explicitly break symmetry. Here the number of components ψ_i is not dictated by the broken symmetry pattern. Multicomponent GL expansions can be justified when, for example, $SU(N)$ or $[U(1)]^N$ symmetry is softly explicitly broken down to $U(1)$ [18]. Recently, rigorous mathematical work has been done on the justification of multicomponent Ginzburg–Landau expansions [19]. Some generalizations of type-1.5 concepts for the case of p-wave pairing in multiband systems were discussed in [20].

4.1.1 Type-1.5 superconductivity

Multicomponent systems allow a type of superconductivity that is distinct from type-1 and type-2 [7, 10, 18, 21–26]. It emerges from the following circumstances: Multicomponent GL models have several fundamental scales, namely the magnetic field penetration depth λ and multiple coherence lengths (characteristic scales of the variations of the density fields) ξ_i, which render the model impossible to parameterize in terms of a single dimensionless parameter κ, thus making the type-1/type-2 dichotomy insufficient for classifying and describing these systems. Rather, in a wide range of parameters, there is a separate superconducting regime with some coherence lengths that are larger and some that are smaller than the magnetic field penetration length $\xi_1/\sqrt{2} < \xi_2/\sqrt{2} < \ldots < \lambda < \xi_M/\sqrt{2} < \ldots < \xi_N/\sqrt{2}$. In that regime a situation is possible where vortices exhibit long-range attraction (attributable to overlap of "outer cores") and short-range repulsion (driven by current-current and electromagnetic interaction) and form vortex clusters coexisting with domains of the two-component Meissner state [21]. The first experimental works [25, 26] proposed that this state is realized in the two-band material MgB_2. Moshchalkov et al. termed this regime "type-1.5 superconductivity" [25]. Recently, experimental works proposed that this state is realized in Sr_2RuO_4 [27, 28] and $LaPt_3Si$ [29, 30]. A prediction of a (narrow) region of the type-1.5 state was made for certain interface superconductors [31]. Also it was pointed out that a generic type-1.5 regime should form in certain iron-based superconductors near transitions from s to $s+is$ pairing states [10]. Type-1.5 superconductivity has been discussed in the context of the quantum Hall effect [32] and neutron stars [33]. For other recent works on this and related subjects see e.g., [20, 34–43].

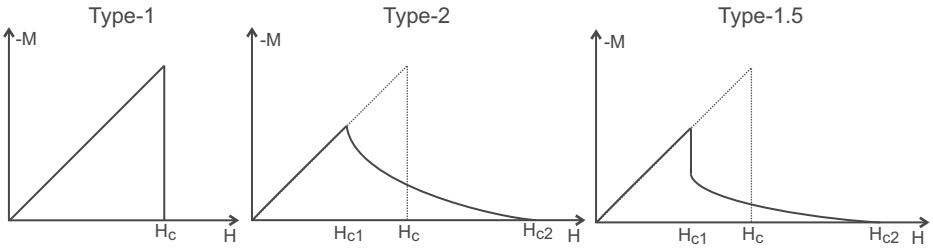

Fig. 4.1: A schematic picture of magnetization curves of type-1, type-2 and type-1.5 superconductors. The magnetization jump at H_{c1} is one of the features of the type-1.5 regime. However, it is not a state-defining property since a jump can be caused by a number of other reasons (microscopic corrections, anisotropies etc) in ordinary type-2 superconductors.

In these systems, one cannot straightforwardly use the usual one-dimensional argument concerning the energy of the superconductor-to-normal state boundary to classify the magnetic response. First of all, the energy per vortex in such a case depends on whether a vortex is placed in a cluster or not. Formation of a single isolated vortex might be energetically unfavorable, while formation of vortex clusters can be favorable, because in a cluster (where vortices are placed in a minimum of the interaction potential), the energy per flux quantum is smaller than that for an isolated vortex. Besides the energy of a vortex in a cluster, there appears an additional characteristic associated with the energy of the boundary of a cluster. In other words for systems with inhomogeneous vortex states there are many different interfaces, some of which have positive and some negative free energy.

We summarize the basic properties of type-1, type-2 and type-1.5 regimes in Table 4.1.

4.2 The two-band Ginzburg–Landau model with arbitrary interband interactions. Definition of the coherence lengths and type-1.5 regime

4.2.1 Free energy functional

Realization of the type-1.5 regime requires at least two superconducting components. In this section we study the type-1.5 regime using the following two-component Ginzburg–Landau (TCGL) free energy functional.

$$F = \frac{1}{2}(D\psi_1)(D\psi_1)^* + \frac{1}{2}(D\psi_2)(D\psi_2)^* - \nu \mathrm{Re}\left\{(D\psi_1)(D\psi_2)^*\right\} + \frac{1}{2}(\nabla \times \mathbf{A})^2 + F_\mathrm{p} \quad (4.2)$$

Here $D = \nabla + ie\mathbf{A}$, and $\psi_i = |\psi_i|e^{i\theta_i}$, $i = 1, 2$, represent two superconducting components. While, in general, two components can have different critical temperatures,

Table 4.1: Basic characteristics of bulk clean superconductors in type-1, type-2 and type-1.5 regimes. Here the most common units are used in which the value of the GL parameter which separates type-1 and type-2 regimes in a single-component theory is $\kappa_c = 1/\sqrt{2}$. Magnetization curves in these regimes are shown in Figure 4.1

	Single-component type-1	**Single-component type-2**	**Multi-component type-1.5**
Characteristic lengths scales	Penetration length λ & coherence length ξ ($\frac{\lambda}{\xi} < \frac{1}{\sqrt{2}}$)	Penetration length λ & coherence length ξ ($\frac{\lambda}{\xi} > \frac{1}{\sqrt{2}}$)	Multiple characteristic density variations length scales ξ_i, and penetration length λ, the nonmonotonic vortex interaction occurs in these systems in a large range of parameters when $\xi_1 \leq \xi_2 \leq \ldots < \sqrt{2}\lambda < \xi_M \leq \ldots \leq \xi_N$
Intervortex interaction	Attractive	Repulsive	Attractive at long range and repulsive at short range
Energy of superconducting/normal state boundary	Positive	Negative	Under quite general conditions negative energy of superconductor/normal interface inside a vortex cluster but positive energy of the vortex cluster's boundary
The magnetic field required to form a vortex	Larger than the thermodynamical critical magnetic field	Smaller than the thermodynamical critical magnetic field	In different cases either (i) smaller than the thermodynamical critical magnetic field or (ii) larger than the critical magnetic field for single vortex but smaller than the critical magnetic field for a vortex cluster of a certain critical size
Phases in external magnetic field	(i) Meissner state at low fields, (ii) Macroscopically large normal domains at elevated fields. First-order phase transition between superconducting (Meissner) and normal states	(i) Meissner state at low fields, (ii) vortex lattices/liquids at larger fields. Second-order phase transitions between Meissner and vortex states and between vortex and normal states at the level of mean-field theory.	(i) Meissner state at low fields, (ii) Macroscopic phase separation into vortex clusters coexisting with Meissner domains at intermediate fields, (iii) Vortex lattices/liquids at larger fields. Vortices form via a first-order phase transition. The transition from vortex states to normal state is second order.
Energy $E(N)$ of N-quantum axially symmetric vortex solutions	$\frac{E(N)}{N} < \frac{E(N-1)}{N-1}$ for all N. Vortices collapse onto a single N-quantum mega-vortex	$\frac{E(N)}{N} > \frac{E(N-1)}{N-1}$ for all N. N-quantum vortex decays into N infinitely separated single-quantum vortices	There is a characteristic number N_c such that $\frac{E(N)}{N} < \frac{E(N-1)}{N-1}$ for $N < N_c$, while $\frac{E(N)}{N} > \frac{E(N-1)}{N-1}$ for $N > N_c$. N-quantum vortices decay into vortex clusters.

in the simplest case, the two-band superconductor breaks only $U(1)$ symmetry. Then Equation (4.2) can be obtained as an expansion of the free energy in small gaps and small gradients [17, 18, 44–47]. Such an expansion should not be confused with the simplest expansion in a single small parameter $\tau = (1 - T/T_c)$ that yields only one order parameter for a $U(1)$ system and neglects the second coherence length. The multiparameter expansions that are not based on symmetry are justified under certain conditions [18, 47]. Indeed the existence of two bands in a superconductor by itself is not a sufficient condition for a superconductor to be described by a model like (4.2), with two well-defined coherence lengths. For discussion of the applicability conditions of the theory (4.2) for two-band $U(1)$ systems see [18, 23]. Note that, in a general two-band expansion, the terms corresponding to one component can be larger than terms contributed by another component. However, as will be clear below, for the discussion of typology of superconductors, the relevant parameters are characteristic length scales associated with the exponential laws at which field components restore their ground state values away from a perturbation such as a vortex core (i.e., the coherence lengths). Indeed a component with *smaller amplitude* can give rise to a *longer coherence length* that is important for intervortex interaction, and should not be discarded based merely on the smallness of amplitude $|\psi_i|$. In principle, for the component with larger amplitude, one can keep higher power terms in the GL expansion such as $|\psi_i|^6$, etc. These terms lead to some corrections to the two coherence lengths, while not affecting the overall form of intervortex forces. Typically these terms can be neglected. This can be seen from the comparison of vortex solutions in the GL formalism and in a microscopic model without GL expansion [18].

We begin with the most general analysis by considering the case where F_p can contain an *arbitrary* collection of nongradient terms, or arbitrary power representing various inter- and intraband interactions. Below we show how three characteristic length scales are defined in this two-component model (two associated with density variations and the London magnetic field penetration length).

The only vortex solutions of the model (4.2) which have finite energy per unit length are the integer N-flux quantum vortices which have the following phase windings along a contour l around the vortex core: $\oint_l \nabla\theta_1 = 2\pi N$, $\oint_l \nabla\theta_2 = 2\pi N$, which can be denoted as (N, N). Vortices with differing phase windings (N, M) carry a fractional multiple of the magnetic flux quantum and have energy divergent with the system size [48], which, under usual conditions, makes them irrelevant for the physics of magnetic response.

In what follows, we investigate only the integer flux vortex solutions, which are the energetically cheapest objects to produce by means of an external field in a bulk superconductor. Note that since this object is essentially a bound state of two vortices, it in general will have two different co-centered cores.

4.3 Coherence lengths and intervortex forces at long range in multiband superconductors

In this section we give a criterion for attractive or repulsive force between well-separated vortices in system (4.2) and show how it can be determined purely by analyzing $F_{\rm p}$ and how three fundamental length scales can be defined in the model (4.2) following [7, 22, 49]. We also discuss the condition for nonmonotonic intervortex forces. Below we will analyze system (4.2) in the case $\nu = 0$ but for an arbitrary effective potential. Detailed discussion of the effects of mixed gradient terms can be found in [7]. By gauge invariance, $F_{\rm p}$ may depend only on $|\psi_1|$, $|\psi_2|$ and $\delta = \theta_1 - \theta_2$. We consider the regime when $F_{\rm p}$ has a global minimum at some point other than the one with $|\psi_i| = 0$, namely at $(|\psi_1|, |\psi_2|, \delta) = (u_1, u_2, 0)$ where $u_1 > 0$ and $u_2 \geq 0$ (for discussion of phase-separated regimes see [42]). Then the model has a trivial solution, $\psi_1 = u_1$, $\psi_2 = u_2$, $A = 0$, (i.e., the ground state). Here we are interested in models that support axially symmetric single-vortex solutions of the form

$$\psi_i = f_i(r)e^{i\theta}\,, \quad (A_1, A_2) = \frac{a(r)}{r}(-\sin\theta, \cos\theta) \tag{4.3}$$

where f_1, f_2, a are real profile functions with boundary behavior $f_i(0) = a(0) = 0$, $f_i(\infty) = u_i$, $a(\infty) = -1/e$. No explicit expressions for f_i, a are known, but, by analyzing the system of differential equations they satisfy, one can construct asymptotic expansions for them at large r, see [7, 22].

At large r from the vortex in the model (4.2) the system recovers (up to exponentially small corrections) the ground state. In fact, the long-range field behavior of a vortex solution can be identified with a solution of the linearization of the model about the ground state, in the presence of appropriate point sources at the vortex positions. This idea is explained in detail for single component GL theory in [50]. A common feature of topological solitons (vortices being a particular example) is that the forces they exert on one another coincide asymptotically (at large separation) with those between the corresponding point-like perturbations (point sources) interacting via the linearized field theory [51]. For (4.2), the linearization has one vector ($\boldsymbol{A}$) and three real scalar ($\epsilon_1 = |\psi_1| - u_1$, $\epsilon_2 = |\psi_2| - u_2$ and δ) degrees of freedom. The isolated vortex solutions have, by definition within the ansatz we use, $\delta \equiv 0$ everywhere. Note that the GL system may also possess nonaxially symmetric solutions, such as vortex clusters, and for these there is no reason why δ should vanish everywhere and in fact it does not [24]. However, below we first consider **long-range intervortex** forces within linear approximation where these effects are neglected. In this case, for a single vortex, we can use an axially symmetric ansatz. Hence we have no source for δ, so we can set $\delta = 0$ in the linearization, which becomes

$$F_{\rm lin} = \frac{1}{2}|\nabla\epsilon_1|^2 + \frac{1}{2}|\nabla\epsilon_2|^2 + \frac{1}{2}\begin{pmatrix}\epsilon_1\\ \epsilon_2\end{pmatrix}\cdot\mathcal{H}\begin{pmatrix}\epsilon_1\\ \epsilon_2\end{pmatrix} + \frac{1}{2}(\partial_1 A_2 - \partial_2 A_1)^2 + \frac{1}{2}e^2\left(u_1^2 + u_2^2\right)|A|^2\,. \tag{4.4}$$

Here, $\mathcal{H}$ is the Hessian matrix of $F_{\rm p}(|\psi_1|, |\psi_2|, 0)$ about (u_1, u_2), that is,

$$\mathcal{H}_{ij} = \left.\frac{\partial^2 F_{\rm p}}{\partial|\psi_i|\partial|\psi_j|}\right|_{(u_1,u_2,0)} . \tag{4.5}$$

Note that, in $F_{\rm lin}$, the vector potential field A decouples from the scalar fields ψ_i. This mode mediates a repulsive force between vortices (originating in current-current and magnetic interaction) with decay length which is the London magnetic field penetration length $\lambda = 1/\mu_A$, where μ_A is the mass of the field, that is,

$$\mu_A = e\sqrt{u_1^2 + u_2^2} . \tag{4.6}$$

By contrast, the scalar fields ϵ_1, ϵ_2 are, in general, coupled (i.e., the symmetric matrix $\mathcal{H}$ has off-diagonal terms). To remove the cross-terms one should find a proper linear combination of the fields that correspond to normal modes of the system. To this end we make a linear redefinition of fields, expanding $(\epsilon_1, \epsilon_2)^{\rm T}$ with respect to the orthonormal basis for $\mathbb{R}^2$ formed by the eigenvectors v_1, v_2 of $\mathcal{H}$,

$$(\epsilon_1, \epsilon_2)^{\rm T} = \chi_1 v_1 + \chi_2 v_2 . \tag{4.7}$$

The corresponding eigenvalues μ_1^2, μ_2^2 are necessarily real (since $\mathcal{H}$ is symmetric) and positive (since (u_1, u_2) is a minimum of $F_{\rm p}$), and hence

$$F_{\rm lin} = \frac{1}{2}\sum_{a=1}^{2}\left(|\nabla\chi_i|^2 + \mu_i^2\chi_i^2\right) + \frac{1}{2}(\partial_1 A_2 - \partial_2 A_1)^2 + \frac{1}{2}e\left(u_1^2 + u_2^2\right)|A|^2 . \tag{4.8}$$

The scalar fields χ_1, χ_2 describe linear combinations of the original density fields. The new fields recover ground state values at different characteristic length scales. The characteristic length scales are nothing but coherence lengths which are given by the inverse of μ_i

$$\xi_1 \equiv 1/\mu_1 , \quad \xi_2 \equiv 1/\mu_2 \tag{4.9}$$

respectively. Note that *here and below we absorb a factor* $1/\sqrt{2}$ *in the definition of coherence length*. Each of these fields defines a vortex core of some characteristic size that mediate an attractive force between vortices at long range. In terms of the normal-mode fields χ_1, χ_2 and A, the composite point source which must be introduced into $F_{\rm lin}$ to produce field configurations identical to those of the vortex asymptotics is

$$\kappa_1 = q_1\delta(x) , \quad \kappa_2 = q_2\delta(x) , \quad \mathbf{j} = m(\partial_2, -\partial_1)\delta(x) , \tag{4.10}$$

where κ_1 is the source for χ_1, κ_2 the source of χ_2, $\mathbf{j}$ the source for $\mathbf{A}$, $\delta(x)$ denotes the two-dimensional Dirac delta function and q_1, q_2 and m are unknown real constants which can, in principle, be determined numerically by a careful analysis of the vortex asymptotics. Physically, a vortex, as seen from a long distance can be thought of as a point particle carrying two different types of scalar monopole charge, q_1, q_2, inducing fields of mass μ_1, μ_2 respectively, and a magnetic dipole moment m oriented

orthogonal to the x_1x_2 plane, inducing a massive vector field of mass $\mu_A \equiv (\sqrt{2}\lambda)^{-1}$. The interaction energy experienced by a pair of point particles carrying these sources, held distance r apart, is easily computed in linear field theory. For example, two scalar monopoles of charge q inducing fields of mass μ held at positions $\mathbf{y}$ and $\tilde{\mathbf{y}}$ in $\mathbb{R}^2$ experience interaction energy

$$E_{\rm int} = -\int_{\mathbb{R}^2} \kappa\tilde{\chi} = -\int_{\mathbb{R}^2} q\delta(\mathbf{x}-\mathbf{y})\frac{q}{2\pi}K_0(\mu|\mathbf{y}-\tilde{\mathbf{y}}|) = -\frac{q^2}{2\pi}K_0(\mu|\mathbf{y}-\tilde{\mathbf{y}}|) \tag{4.11}$$

where κ is the source for the monopole at $\mathbf{y}$, $\tilde{\chi}$ is the scalar field induced by the monopole at $\tilde{\mathbf{y}}$ [50] and K_0 denotes the modified Bessel's function of the second kind. The interaction energy for a pair of magnetic dipoles may be computed similarly. In the case of our two-component GL model, the total long-range intervortex interaction energy has three terms, corresponding to the three sources in the composite point source (4.10), and turns out to be

$$E_{\rm int} = \frac{m^2}{2\pi}K_0(\mu_A r) - \frac{q_1^2}{2\pi}K_0(\mu_1 r) - \frac{q_2^2}{2\pi}K_0(\mu_2 r)\,. \tag{4.12}$$

Note that, the first term in this formula, which originates in magnetic and current-current interaction, is repulsive, while the other two are associated with core-core interactions of two kinds of cores and are attractive. The linearized theory does not contain information about the prefactors q_1, q_2 and m. However, they can be determined numerically from the full nonlinear GL theory. At very large r, $E_{\rm int}(r)$ is dominated by whichever term corresponds to the smallest of the three masses, μ_A, μ_1, μ_2, so to determine whether vortices attract at long range, it is enough to compute just these masses. The generalization to the case with a larger number of components is straightforward: additional coherence lengths give additional contributions to attractive interaction in the form $-\frac{q_i^2}{2\pi}K_0(\mu_i r)$. Generalizations to multiple repulsive length scales in layered systems or caused by stray fields were discussed in [38]. In thin films, intervortex interaction acquires also $1/r$ repulsion at long range due to the magnetic field outside the sample, similarly to the single-component case [52].

Consider the case where the long-range interaction is attractive due to $\xi_1 > \lambda > \xi_2$ being the largest length scale of the problem. For the existence of short-range repulsive but long-range attractive interaction it is required that m^2 is sufficiently large. This criterion is equivalent to the condition that the system has a solution with negative free energy interfaces in external fields [7, 22, 49]. Indeed when the interface energy is always positive, the system exhibits type-1 behavior: i.e., tends to form a single vortex with high winding number. If there are interfaces with negative energy in the external field, the system tends to maximize these interfaces. In the type-1.5 regime the system forms vortex clusters, where it maximizes the number of vortex cores inside the vortex clusters. At the same time the system minimizes the interface of the cluster itself (that costs positive energy).

To summarize, the nature of intervortex forces at large separation in the model under consideration, can be determined purely by analyzing $F_{\rm p}$: one finds the ground state (u_1, u_2) and the Hessian $\mathcal{H}$ of $F_{\rm p}$ about (u_1, u_2). From this one computes the mass of the vector field A, $\mu_A = e\sqrt{u_1^2 + u_2^2}$ (i.e., the inverse of the magnetic field penetration length), and the masses μ_1, μ_2 of the scalar normal modes (i.e., the inverses of the coherence lengths), these masses being the square roots of the eigenvalues of $\mathcal{H}$. If either (or both) of μ_1, μ_2 are less than μ_A, then the dominant interaction at long range is attractive (i.e., the vortex core extends beyond the area where the magnetic field is localized), while if μ_A is less than both μ_1 and μ_2, the dominant interaction at long range is repulsive. The special feature of the two-component model is that the vortices whose core extends beyond the magnetic field penetration length are thermodynamically stable in a range of parameters and, moreover, one can have a repulsive force between the vortices at shorter distances where the system has thermodynamically stable vortex solutions [7, 22, 49]. It is important to stress that length scales μ_1^{-1}, μ_2^{-1} are not directly associated with the individual condensates ψ_1, ψ_2. Rather they are associated with the normal modes χ_1, χ_2, defined as [7, 22]

$$\chi_1 = (|\psi_1| - u_1)\cos\Theta - (|\psi_2| - u_2)\sin\Theta\,, \quad \chi_2 = -(|\psi_1| - u_1)\sin\Theta - (|\psi_2| - u_2)\cos\Theta\,. \tag{4.13}$$

These may be thought of as rotated (in field space) versions of $\epsilon_1 = |\psi_1| - u_1$, $\epsilon_2 = |\psi_2| - u_2$. The *mixing angle*, that is, the angle between the χ and ϵ axes, is Θ, where the eigenvector v_1 of $\mathcal{H}$ is $(\cos\Theta, \sin\Theta)^{\rm T}$. This, again, can be determined directly from $\mathcal{H}$.

Note also that the shorter of the length scales μ_1^{-1}, μ_2^{-1}, although being a fundamental length scale of the theory, can be masked in a density profile of a vortex solution by nonlinear effects. This, for example certainly happens if $\mu_1^{-1} \ll \mu_A \equiv \lambda^{-1}$ (see short discussion in Ref. [22]). Also note that in general the minimum of the interaction potential will not be located at the London penetration length, because it will in general also be affected by nonlinearities. From this discussion it follows that, in general, one cannot drop the subdominant component based on comparison of the ground state values of the amplitudes of $|\psi_i|$ in the GL expansion. Namely, the long-range interaction can be determined by a mode with smaller amplitude. The formal justification of the multiband GL expansion can be found in [18].

4.4 Critical coupling (Bogomol'nyi point)

In single-component superconductors, the type-1 and type-2 regimes are separated by a **Bogomol'nyi point** $\kappa = 1$ (note that above we absorbed the factor $1/\sqrt{2}$ into the definition of coherence length). At that point, vortices do not interact, the free energy of normal-to-superconductor interfaces is zero and we have $H_{\rm c1} = H_{\rm c2} = H_{\rm c}$ [5, 51, 53, 54]. This regime is referred to as the "critical point" because of the saturation of the Bogomol'nyi inequality [5, 51, 53–56]. The necessary, but not sufficient, conditions for a crit-

ical point is lack of intervortex forces at long range within the linear approximation. To that end, all modes excited in a vortex solution must have equal masses μ_i and amplitudes. From Equation (4.12) it is obvious that for a multicomponent superconductor it requires fine tuning and, in general, type-1 and type-2 regimes are not separated by a critical point. Furthermore, from the section on microscopic theory below, it is clear that in general μ_1 and μ_2 (as functions of the system's parameters) do not cross but form an avoided crossing. Thus, in the two-component case the Bogomol'nyi critical point is a zero-measure parameter set which requires special symmetry of the model. Such fine tuning for a composite vortex can be achieved in a $U(1) \times U(1)$ system with a potential that is symmetric with respect to both components

$$F_{\mathrm{p}} = -\alpha|\psi_1|^2 + \frac{\beta}{2}|\psi_1|^2 - \alpha|\psi_2|^2 + \frac{\beta}{2}|\psi_2|^2 \tag{4.14}$$

For a standard form of gradient terms, this potential gives equal coherence lengths. The Bogomol'nyi point is realized when $\xi_1 = \xi_2 = \lambda$. Just like in a single-component system, vortices do not interact in this regime. In single-component superconductors with $\kappa \approx 1$, a substantial literature was devoted to intervortex interactions that appear beyond Ginzburg–Landau field theory in microscopic theory [6, 57, 58]. As follows from the microscopic theory of multiband systems [23], these effects are in general negligible for the type-1.5 regime. The microscopic theory [23] confirms that the physics behind the vortex interaction in the type-1.5 regime is dominated by the same mechanism as in the GL model: density-density interaction caused by a large "outer core" due to a disparity in coherence lengths.

4.5 Microscopic theory of type-1.5 superconductivity in $U(1)$ multiband case

In this section we briefly outline microscopic theory of type-1.5 superconductivity in the particular case of multiband superconductors that break only $U(1)$ symmetry. In this case existence of multiple coherence lengths does not follow from symmetry and has to be justified. A reader who is interested in more general cases of higher symmetry breaking as well as the general properties of the type-1.5 state can skip this discussion and proceed directly to the next section. Existence of multiple superconducting bands is not a necessary condition for appearance of multiple coherence lengths [23]. The appearance of multiple coherence lengths and a type-1.5 regime in multiband-band superconductors was described using microscopic theory at all temperatures, without relying on GL expansions in [23]. We refer a reader, interested in a full microscopic theory that does not rely on GL expansion to that work, while here we focus on microscopic justification of GL expansion.

As discussed above, in multiband systems, in general multicomponent GL expansions are not based on symmetry. Therefore, obviously it cannot be obtained as an

expansion in a single small parameter $\tau = 1 - T/T_c$. Instead such expansions are justified when the system has multiple small parameters which are not symmetry-related. In the simplest case these are multiple small gaps in different bands, small gradients, and small interband coupling constants. A single-parameter-τ expansion emerges as a single-component reduction of the model in the $\tau \to 0$ limit for a system that breaks only $U(1)$ symmetry [18].

In this section we focus on the two-band case and consider the microscopic derivation of the two-component GL model (TCGL):

$$F = \sum_{j=1,2} \left(a_j |\Delta_j|^2 + \frac{b_j}{2} |\Delta_j|^4 + K_j |\boldsymbol{D}\Delta_j|^2 \right) - \gamma \left(\Delta_1 \Delta_2^* + \Delta_2 \Delta_1^* \right) + \frac{B^2}{8\pi} \tag{4.15}$$

where $\boldsymbol{D} = \nabla + i\boldsymbol{A}$, $\boldsymbol{A}$ and $\boldsymbol{B}$ are the vector potential and magnetic field and $\Delta_{1,2}$ are the gap functions in two different bands.

4.5.1 Microscopic Ginzburg–Landau expansion for $U(1)$ two-band system

To verify applicability of TCGL theory we consider the microscopic model of a clean superconductor with two overlapping bands at the Fermi level [18, 23]. Within quasiclassical approximation the band parameters characterizing the two different cylindrical sheets of the Fermi surface are the Fermi velocities $V_{\mathrm{F}j}$ and the partial densities of states (DOS) ν_j, labeled by the band index $j = 1, 2$.

It is convenient to normalize the energies to the critical temperature T_c and length to $r_0 = \hbar V_{\mathrm{F}1}/T_c$. The vector potential is normalized by $\phi_0/(2\pi r_0)$, the current density normalized by $c\phi_0/(8\pi^2 r_0^3)$ and therefore the magnetic field is measured in units $\phi_0/(2\pi r_0^2)$ where $\phi_0 = \pi\hbar c/e$ is the magnetic flux quantum. In these units the Eilenberger equations for quasiclassical propagators take the form

$$\begin{aligned} v_{\mathrm{F}j} \boldsymbol{n}_{\mathrm{p}} \boldsymbol{D} f_j + 2\omega_n f_j - 2\Delta_j g_j = 0 \,, \\ v_{\mathrm{F}j} \boldsymbol{n}_{\mathrm{p}} \boldsymbol{D}^* f_j^+ - 2\omega_n f_j^+ + 2\Delta_j^* g_j = 0 \,. \end{aligned} \tag{4.16}$$

Here $v_{\mathrm{F}j} = V_{\mathrm{F}j}/V_{\mathrm{F}1}$, $\omega_n = (2n+1)\pi T$ are Matsubara frequencies, the vector $\boldsymbol{n}_{\mathrm{p}} = (\cos\theta_{\mathrm{p}}, \sin\theta_{\mathrm{p}})$ parameterizes the position on 2D cylindrical Fermi surfaces. The quasiclassical Green's functions in each band obey the normalization condition $g_j^2 + f_j f_j^+ = 1$.

The self-consistency equation for the gaps is

$$\Delta_i = T \sum_{n=0}^{N_{\mathrm{d}}} \int_0^{2\pi} \lambda_{ij} f_j \, d\theta_{\mathrm{p}} \,. \tag{4.17}$$

The coupling matrix λ_{ij} satisfies the symmetry relations $n_1\lambda_{12} = n_2\lambda_{21}$ where n_i are the partial densities of states normalized so that $n_1 + n_2 = 1$. The vector potential

satisfies the Maxwell equation $\nabla \times \nabla \times \boldsymbol{A} = \boldsymbol{j}$ where the current is

$$\boldsymbol{j} = -T \sum_{j=1,2} \sigma_j \sum_{n=0}^{N_d} \mathrm{Im} \int_0^{2\pi} \boldsymbol{n}_p g_j d\theta_p \,. \tag{4.18}$$

The parameters σ_j are given by $\sigma_j = 4\pi\rho n_j v_{Fj}$ and

$$\rho = (2e/c)^2 (r_0 V_{F1})^2 \nu_0 \,.$$

Here we briefly outline the derivation of the TCGL functional (4.15) from the microscopic equations following [23]. First we find the solutions of the Eilenberger equations (4.16) in the form of the expansion by the gap functions amplitudes $|\Delta_{1,2}|$ and their gradients $|(\boldsymbol{n}_p \boldsymbol{D})\Delta_{1,2}|$. Then these solutions are substituted to the self-consistency equation (4.17). Using this procedure we find the solutions of Equations (4.16) in the form:

$$f_j = \frac{\Delta_j}{\omega_n} - \frac{|\Delta_j|^2 \Delta_j}{2\omega_n^3} - \frac{v_{Fj}}{2\omega_n^2}(\boldsymbol{n}_p \boldsymbol{D})\Delta_j + \frac{v_{Fj}^2}{4\omega_n^3}(\boldsymbol{n}_p \boldsymbol{D})(\boldsymbol{n}_p \boldsymbol{D})\Delta_j \,, \tag{4.19}$$

and $f_j^+(\boldsymbol{n}_p) = f_j^*(-\boldsymbol{n}_p)$. Note that this GL expansion is based on neglecting the higher order terms in powers of $|\Delta|$ and $|(\boldsymbol{n}_p \boldsymbol{D})\Delta|$. Indeed this approximation naturally fails in a number of cases. The regimes when it can be justified were determined in the work [18] by a direct comparison to the full microscopic model. Let us determine microscopic coefficients in the GL expansion. Substituting to the self-consistency equations (4.17) and integrating by θ_p we obtain

$$\Delta_1 = (\lambda_{11}\Delta_1 + \lambda_{12}\Delta_2)G + (\lambda_{11} GL_1 + \lambda_{12} GL_2) \tag{4.20}$$

$$\Delta_2 = (\lambda_{21}\Delta_1 + \lambda_{22}\Delta_2)G + (\lambda_{21} GL_1 + \lambda_{22} GL_2) \tag{4.21}$$

where

$$G = 2 \sum_{n=0}^{N_d} \frac{\pi T}{\omega_n} \,; \quad X = \sum_{n=0} \frac{\pi T}{\omega_n^3} \tag{4.22}$$

$$GL_j = X \left(\frac{v_{Fj}^2}{4} \boldsymbol{D}^2 \Delta_j - |\Delta_j|^2 \Delta_j \right) \tag{4.23}$$

Expressing GL_i from the equations above we obtain

$$n_1 GL_1 = n_1 \left(\frac{\lambda_{22}}{\mathrm{Det}\hat{\lambda}} - G \right) \Delta_1 - \frac{\lambda_J n_1 n_2}{\mathrm{Det}\hat{\lambda}} \Delta_2 \tag{4.24}$$

$$n_2 GL_2 = n_2 \left(\frac{\lambda_{11}}{\mathrm{Det}\hat{\lambda}} - G \right) \Delta_2 - \frac{\lambda_J n_1 n_2}{\mathrm{Det}\hat{\lambda}} \Delta_1 \tag{4.25}$$

The system of two coupled GL Equations (4.24) can be obtained minimizing the free energy provided the coefficients in Equation (4.15) are given by

$$\begin{aligned} a_i &= \rho n_i(\tilde{\lambda}_{ii} + \ln T - G_c) \\ \gamma &= \rho n_1 n_2 \lambda_J / \mathrm{Det}\hat{\lambda} \\ b_i &= \rho n_i X / T^2 \\ K_i &= v_{Fi}^2 b_i / 4 \end{aligned} \tag{4.26}$$

where $\lambda_J = \lambda_{21}/n_1 = \lambda_{12}/n_2$. Note that the expression for K_i in Ref. [18] has an extra coefficient ρ. The temperature is normalized to T_c. Here $X = 7\zeta(3)/(8\pi^2) \approx 0.11$, $\bar{\lambda}_{ij} = \lambda_{ij}^{-1}$ and $G_c = G(T_c)$ is determined by the minimal positive eigenvalue of the inverse coupling matrix $\hat{\lambda}^{-1}$:

$$G_c = \frac{\mathrm{Tr}\lambda - \sqrt{\mathrm{Tr}\lambda^2 - 4\mathrm{Det}\lambda}}{2\mathrm{Det}\lambda} .$$

We have used the expression $G(T) = G(T_c) - \ln T$. Near the critical temperature $\ln T \approx -\tau$ and we obtain

$$a_i = \alpha_i(T - T_i) \tag{4.27}$$

$$\alpha_i = n_i \lambda_J \tag{4.28}$$

$$T_i = (1 + G_c - \tilde{\lambda}_{ii}) . \tag{4.29}$$

In the above procedure of GL expansion leading to system (4.24) we assumed both the eigenvalues of the coupling matrix $\hat{\lambda}$ are positive.

4.5.2 Temperature dependence of coherence lengths

Coherence lengths are given by the inverse masses of linear modes. First we investigate the asymptotic behavior of the superconducting gaps formulated in terms of the linear modes of the density fields both in TCGL and microscopic theories described in the previous section. To find the linear modes we follow the procedure described in Section 4.3 using the GL model with expansion coefficients (4.26). Let us set $K_1 = K_2$ which can be accomplished by rescaling the fields $\Delta_{1,2}$. Then the corresponding Hessian matrix (4.5) can be diagonalized with the k-independent rotation introducing the normal modes $\chi_\beta = U_{\beta i}(\Delta_i - \Delta_{i0})$ where $\beta = L, H$ and $i = 1, 2$. The rotation matrix $\hat{U}$ is characterized by the mixing angle [7, 23] as follows:

$$\hat{U} = \begin{pmatrix} \cos\theta_L & \sin\theta_L \\ -\sin\theta_H & \cos\theta_H \end{pmatrix} \tag{4.30}$$

Note that in accordance with the results of section (4.3) the TCGL theory yields identical values of two mixing angles $\theta_L = \theta_H = \Theta$. However, in general, outside the region

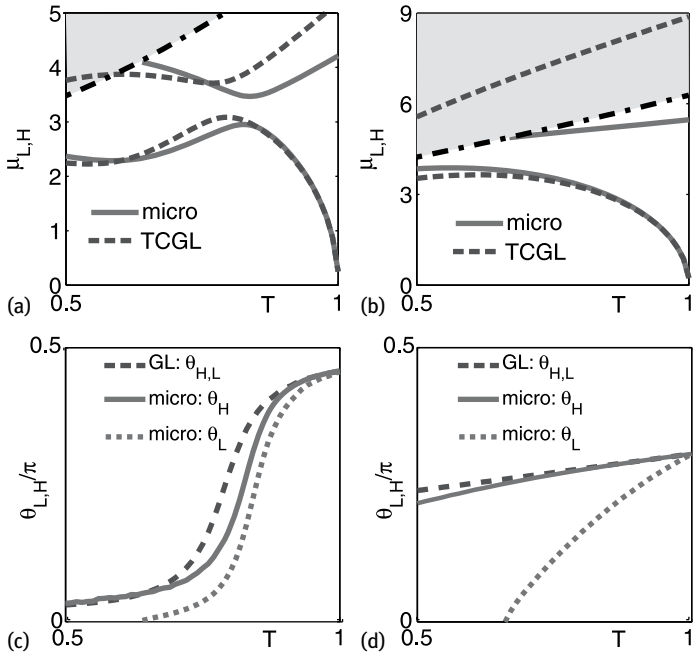

Fig. 4.2: (a) and (b) Comparison of field masses (inverse coherence lengths) given by full microscopic (solid lines), and microscopically derived TCGL (dotted) theories. The microscopic parameters are $\lambda_{11} = 0.5$, $\lambda_{22} = 0.426$ and $\lambda_{12} = \lambda_{21} = 0.01;\ 0.1$ for (a,b) respectively. The yellow shaded region above the dashed-dotted line shows the continuum of length scales determined by branch-cut contributions which are specific to the microscopic theory and are not captured by the TCGL description. (c,d) Comparison of mixing angle behavior given by the exact microscopic (red lines) and microscopically derived TCGL theories (blue line). Note that the larger coherence length has a maximum as a function of temperature deep below T_c near the crossover to the regime when the weak band superconductivity is induced by an interband proximity effect (the corresponding inverse quantity μ_L has a minimum). This nonmonotonic coherence length behavior is more pronounced at weak interband coupling and disappears at strong interband coupling [23]. A multiband system with weak interband interaction can easily fall into the type-1.5 regime near that crossover temperature. Panels (b) and (d) show how the TCGL theory starts to deviate from microscopic theory at lower temperatures when interband coupling is increased. Parameters are the same as on panels (a,b) respectively.

where GL expansion is accurate, the exact microscopic calculation yields deviations $\theta_H \neq \theta_L$. This is discussed in Ref. [18].

The fields $\chi_{L,H}$ corresponding to the linear combinations of $\Delta_{1,2}$ vary at distinct lengths: $\xi_H = 1/\mu_H$ and $\xi_L = 1/\mu_L$. They constitute coherence lengths of the TCGL theory (4.15) and characterize the asymptotic relaxation of the linear combinations of the fields $\Delta_{1,2}$, the linear combinations are represented by the composite fields $\chi_{L,H}$.

With the help of Equations (4.26) for GL coefficients obtained from microscopic theory we can study the temperature dependencies of the coherence lengths char-

acterizing the asymptotic relaxation of the gap fields. Since the system in question breaks only one symmetry, then at critical temperature only one coherence length can diverge while the second coherence should stay finite. Infinitesimally close to critical temperature $T = T_c - 0$ the divergent coherence length has the following standard mean-field behavior $\xi_L = 1/\mu_L \sim 1/\tau^{1/2}$, where $\tau = 1 - T/T_c$. The contribution of another linear mode in the theory sets the scale which is proportional to $\xi_H = 1/\mu_H$ and remains finite even at $T = T_c$. But the amplitude of this mode rapidly vanishes in the region $T = T_c - 0$. Similar behavior can be derived directly in a full microscopic calculation [18]. In Figure 4.2a, b the temperature dependence of masses $\mu_{L,H}$ is plotted comparing the results of the full microscopic [23] and microscopically derived TCGL theories [18]. It is shown for the cases of weak and strong interband coupling in Figure 4.2c, d. We have found that TCGL theory describes the lowest characteristic mass $\mu_L(T)$ with a very good accuracy near T_c (compare the blue and red curves in Figure 4.2a, b). Remarkably, when interband coupling is relatively weak (Figure 4.2c) the "light" mode is quite well described by TCGL also at low temperatures down to $T = 0.5T_c$ around which the weak band crosses over from active to passive (proximity-induced) superconductivity. Indeed the τ parameter is large in that case. Nonetheless, if the interband coupling is small one does have a small parameter to implement a GL expansion for one of the components. Namely, one can still expand, e.g., in the powers of the weak gap $|\Delta_2|/\pi T \ll 1$. Conversely, for the "heavy" mode we naturally obtain some discrepancies even relatively close to T_c, although TCGL theory gives a qualitatively correct picture for this mode when the interband coupling is not too strong. More substantial discrepancies between TCGL and microscopic theories appear only at lower temperatures or at stronger interband coupling (Figure 4.2d) where the microscopic response function has only one pole, while TCGL theory generically has two poles. Note that these expected deviations concern shorter range physics and do not directly affect long-range intervortex forces. In the type-1.5 regime long-range attractive forces are governed by core-core interaction whose range is set by the larger coherence length (lighter mode). The long-range attractive forces here are similar to the long-range forces in type-1 superconductors, while short-range forces are similar to those in type-2 superconductors. These interactions are obviously principally different from microscopic-physics-dominated intervortex forces in superconductors near the Bogomol'nyi point. Most clearly that can be distinguished within the microscopic theory [23].

The microscopic two-band GL expansion discussed in this section has a straightforward generalization to N-component expansions in N-band $U(1)$ models [47], as well as to more complicated states such as $s+is$ that break multiple symmetries [9, 47].

4.6 Systems with generic breakdown of type-1/type-2 dichotomy

The simplest situation where the type-1/type-2 dichotomy generically does not hold are superconducting systems that exhibit a phase transition from the $U(1)$ to $U(1) \times U(1)$ state (or similar transitions between the states with broken higher symmetries), such as the theoretically discussed superconducting states of liquid metallic hydrogen or deuterium [11], or models involving mixture of protonic and Σ^- hyperonic condensates in neutron stars [13]. Indeed at such a transition the magnetic field penetration length remains finite but there is a divergent coherence length due to the breakdown of additional symmetry (if the phase transition is continuous). Also the mode associated with the divergent coherence length looses its amplitude at the phase transition. Therefore, near this transition one of the coherence lengths is the largest length scale of the problem and the system can only be either a type-1 or type-1.5 superconductor. A similar situation was discussed in the context of interface superconductors [31].

In a way similar, but more subtle, situation takes place at the transition from the s to $s + is$ state [10]. The $s + is$ superconductor breaks additional Z_2 symmetry and there is a corresponding diverging coherence length in the problem. An important generic aspect of the $s + is$ superconducting states is that the density excitations are coupled with the phase difference excitations in the linear theory [10]. One of the mixed phase-difference-density modes gives rise to a divergent coherence length at that phase transition. Thus, such a system can be either type-1 or type-1.5 near the transition from the s to $s + is$ state.

4.7 Structure of vortex clusters in the type-1.5 regime in a two-component superconductor

In this section, following Ref. [24], we consider in more detail the full nonlinear problem in two-component Ginzburg–Landau models, with and without Josephson coupling η which directly couples the two condensates (for treatment of other kinds of interband coupling see [7], for microscopic derivation of the coefficients see Section 4.5). When $\eta = 0$ the condensates are coupled electromagnetically. When there is nonzero interband Josephson coupling, the phase difference is associated with a massive mode with mass $\sqrt{\eta(u_1^2 + u_2^2)/u_1 u_2}$.

$$\mathcal{F} = \frac{1}{2} \sum_{i=1,2} \left[|(\nabla + ie\mathbf{A})\psi_i|^2 + \left(2\alpha_i + \beta_i |\psi_i|^2\right) |\psi_i|^2 \right] + \frac{1}{2}(\nabla \times \mathbf{A})^2 - \eta |\psi_1||\psi_2| \cos(\theta_2 - \theta_1) \tag{4.31}$$

Since the Ginzburg–Landau model is nonlinear, in general intervortex interactions are nonpairwise. Nonpairwise interactions are important at shorter ranges where the linearized theory, considered above, does not in general apply. Below we discuss the importance of complicated nonpairwise forces between superconducting vortices

arising in certain cases in multicomponent systems [24, 42, 43]. These nonpairwise forces in certain situations have important consequences for vortex cluster formation in the type-1.5 regime.

Figures 4.3 and 4.4 show numerical solutions for N-vortex bound states in several regimes (for technical details see Appendix of [24]). The common aspect of the regimes shown on these figures is that the density of one of the components is depleted in the vortex cluster and has its current mostly concentrated on the boundary of the vortex cluster (i.e., has a "type-1"-like behavior). At the same time, the second component forms a distinct vortex lattice inside the vortex cluster (i.e., has a "type-2"-like behavior).

When stray fields are taken into account in thin films, they give repulsive intervortex interaction at very long distances, while vortices can retain attractive interaction at intermediate length scales. That gives rise to various hierarchical structures such as lattices of vortex clusters or vortex stripes [38, 59]. The study of dynamics demonstrated that such vortex systems can form a vortex glass phase [60]. This is in contrast

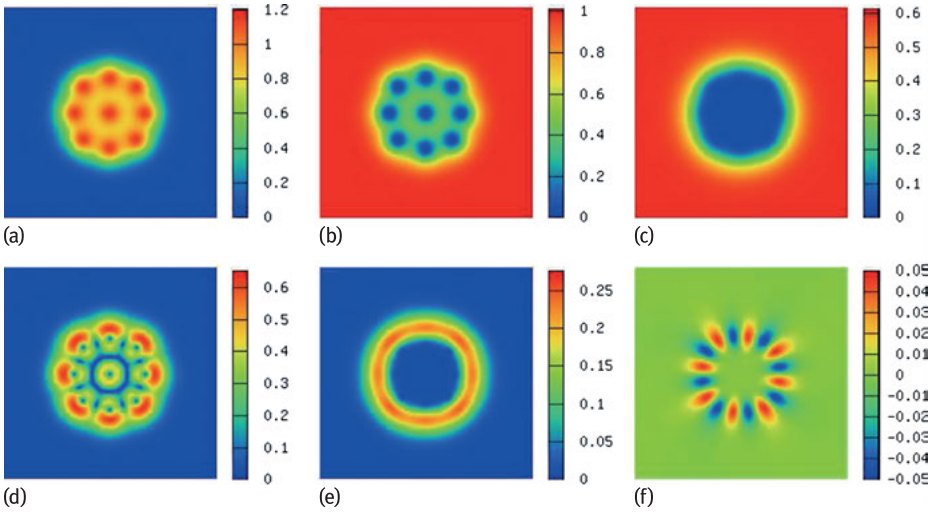

Fig. 4.3: Ground state of $N_v = 9$ flux quanta in a $U(1) \times U(1)$ type-1.5 superconductor (i.e., $\eta = 0$). The parameters of the potential being here $(\alpha_1, \beta_1) = (-1.00, 1.00)$ and $(\alpha_2, \beta_2) = (-0.60, 1.00)$, while the electric charge is $e = 1.48$ (in these units the electric charge value parameterizes the London penetration length). The displayed physical quantities are (a) the magnetic flux density, (b) (*resp.* c) is the density of the first (*resp.* second) condensate $|\psi_{1,2}|^2$. (d) (*resp.* e) shows the norm of the supercurrent in the first (*resp.* second) component. Panel (f) is $\mathrm{Im}(\psi_1^* \psi_2) \equiv |\psi_1||\psi_2| \sin(\theta_2 - \theta_1)$ being nonzero when there appears to be a difference between the phase of the two condensates. The solution shows that clearly there is a vortex interaction-induced phase-difference gradient that contributes to nonpairwise intervortex forces. Parameters are chosen so that the second component has a type-1-like behavior while the first one tends to form well-separated vortices. The density of the second band is depleted in the vortex cluster and its current is mostly concentrated on the boundary of the cluster (see Ref. [24]).

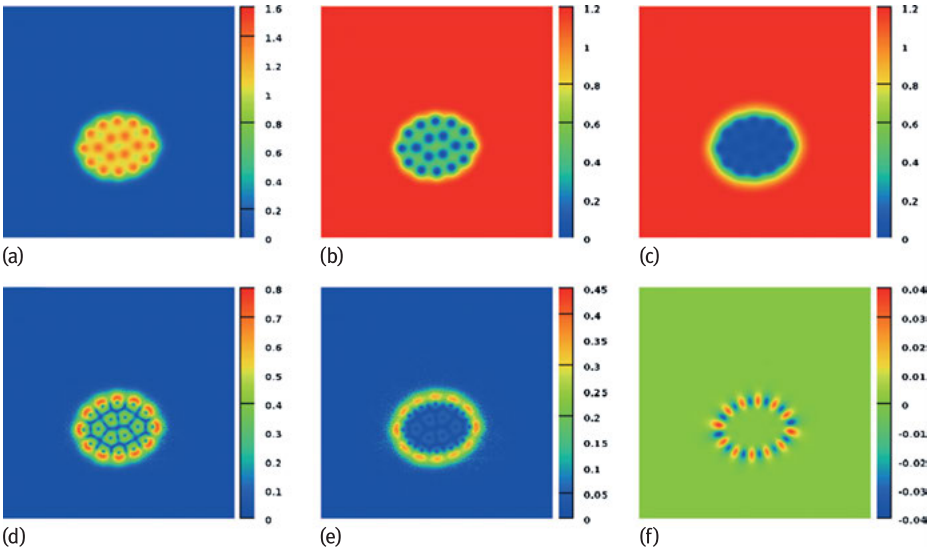

Fig. 4.4: Elongated ground state cluster of 18 vortices in a superconductor with two active bands. Parameters of the interacting potential are $(\alpha_1, \beta_1) = (-1.00, 1.00)$, $(\alpha_2, \beta_2) = (-0.0625, 0.25)$ while the interband coupling is $\eta = 0.5$. The electric charge, parameterizing the penetration depth of the magnetic field, is $e = 1.30$ so that the well in the nonmonotonic interacting potential is very small. In this case there is visible admixture of the current of the second component in vortices inside the cluster, though its current is predominantly concentrated on the boundary of the cluster.

to type-2 superconductors where a vortex glass can appear only in the presence of vortex pinning and not in clean samples.

4.8 Macroscopic separation in domains of different broken symmetries in type-1.5 superconducting state

As discussed above, a system with nonmonotonic intervortex interaction potentials allows a state with macroscopic phase separation in vortex droplets and Meissner domains. In type-1.5 superconductors this state can also represent a phase separation into domains of states with different broken symmetries. In this section we will give two different examples of how such behavior can arise.

Note that in multicomponent superconductors some symmetries are global (i.e., associated with the degrees of freedom decoupled from the vector potential) and some are local, i.e., associated with the degrees of freedom coupled to the vector potential. As is well known, in the latter case the concept of spontaneous symmetry breakdown is not defined the same way as in a system with global symmetry. However below, for

brevity we will not be making terminological distinctions between local and global symmetries (detailed discussion of these aspects can be found in e.g., [48]).

4.8.1 Macroscopic phase separation into $U(1) \times U(1)$ and $U(1)$ domains in the type-1.5 regime

Consider a superconductor with broken $U(1) \times U(1)$ symmetry, i.e., a collection of independently conserved condensates with no intercomponent Josephson coupling. As discussed above, in the vortex cluster state, in the interior of a vortex droplet, the superconducting component which has vortices with larger cores is more depleted. In the $U(1) \times U(1)$ system the vortices with phase windings in different condensates are bound electromagnetically, resulting in an asymptotically logarithmic interaction potential with a prefactor proportional to $|\psi_1|^2|\psi_2|^2/(|\psi_1|^2+|\psi_2|^2)$ [48], and even weaker interaction strength at shorter separations.

Consider now a macroscopically large vortex domain. Even if the second component there is not completely depleted, its density is suppressed and, as a consequence the binding energy between vortices with different phase windings ($\Delta\theta_1 = 2\pi, \Delta\theta_2 = 0$) and ($\Delta\theta_1 = 0, \Delta\theta_2 = 2\pi$), can be arbitrarily small. Moreover, the vortex ordering energy in the component with more depleted density is small as well. As a result, even a tiny thermal fluctuation can drive a vortex sublattice melting transition [11, 61] in a large vortex cluster. In that case the fractional vortices in the weaker component tear themselves off the fractional vortices in the strong component and form a disordered state. Note that vortex sublattice melting is associated with the phase transition from $U(1) \times U(1)$ to $U(1)$ broken symmetries [11, 61]. Thus, a macroscopically large vortex cluster can realize a domain of $U(1)$ phase (associated with the superconducting state of the strong component) immersed in a vortexless $U(1) \times U(1)$ Meissner state domain. If the magnetic field is increased, the system will go from the vortex cluster state (with coexisting $U(1) \times U(1)$ and $U(1)$ domains) to a $U(1)$ vortex state.

4.8.2 Macroscopic phase separation in $U(1)$ and $U(1) \times Z_2$ domains in three-band type-1.5 superconductors

In this subsection we discuss an example of vortex clusters in three-band superconductors that locally break an additional Z_2 symmetry forming "phase-frustrated" states. Such superconductors also allow the coexistence of domains with different broken symmetries in the ground state. The minimal GL free energy functional to model a three-band superconductor is

$$F = \frac{1}{2}(\nabla\times\mathbf{A})^2 + \sum_{i=1,2,3}\frac{1}{2}|\mathbf{D}\psi_i|^2 + \alpha_i|\psi_i|^2 + \frac{1}{2}\beta_i|\psi_i|^4 + \sum_{i=1,2,3}\sum_{j>i}\eta_{ij}|\psi_i||\psi_j|\cos(\varphi_{ij}). \quad (4.32)$$

Here the phase differences between two condensates are denoted $\varphi_{ij} = \theta_j - \theta_i$. Microscopic derivations of such models describing $s + is$ superconducting states can be found in [9, 47].

Systems with more than two Josephson-coupled bands can exhibit *phase frustration* [8–10, 62, 63]. For $\eta_{ij} < 0$, a given Josephson interaction energy term is minimal for zero phase difference (we then refer to the coupling as "phase-locking"), while when $\eta_{ij} > 0$ it is minimal for a phase difference equal to π (we then refer to the coupling as "phase-antilocking"). Two-component systems with bilinear Josephson coupling are symmetric with respect to the sign change $\eta_{ij} \to -\eta_{ij}$ as the phase difference changes by a factor π, for the system to recover the same interaction. However, in systems with more than two bands there is generally no such symmetry. For example, if a three-band system has $\eta > 0$ for all Josephson interactions, then these terms cannot be simultaneously minimized, as this would correspond to all possible phase differences being equal to π.

The ground state values of the fields $|\psi_i|$ and φ_{ij} of system (4.32) are found by minimizing the potential energy

$$\sum_i \left\{ \alpha_i |\psi_i|^2 + \frac{1}{2}\beta_i |\psi_i|^4 \right\} + \sum_{j>i} \eta_{ij} |\psi_i||\psi_j| \cos(\varphi_{ij}) \,. \tag{4.33}$$

This can however not be done analytically in general, though certain properties can be derived from qualitative arguments. In terms of the sign of the η's, there are four principal situations:

Case	Sign of $\eta_{12}, \eta_{13}, \eta_{23}$	Ground state phases
1	$- - -$	$\varphi_1 = \varphi_2 = \varphi_3$
2	$- - +$	Frustrated
3	$- + +$	$\varphi_1 = \varphi_2 = \varphi_3 + \pi$
4	$+ + +$	Frustrated

Case (2) can result in several ground states. If $|\eta_{23}| \ll |\eta_{12}|,\ |\eta_{13}|$, then the phase differences are generally $\varphi_{ij} = 0$. Conversely, if $|\eta_{12}|,\ |\eta_{13}| \ll |\eta_{23}|$ then $\varphi_{23} = \pi$ and φ_{12} is either 0 or π. However, in certain parameter ranges the resulting state is in fact a "compromise" where φ_{ij} is not an integer multiple of π.

Case (4) is in fact equivalent to (2) (mapping between these scenarios is trivial). The wide range of resulting ground states can be seen in Figure 4.5. As η_{12} is scaled, ground state phases change from $(-\pi,\ \pi,\ 0)$ to the limit where one band is depleted and the remaining phases are $(-\pi/2,\ \pi/2)$.

An important property of the potential energy (4.33) is that if any of the phase differences φ_{ij} is not an integer multiple of π, then the ground state possesses an additional discrete Z_2 degeneracy. For example, for a system with $\alpha_i = -1,\ \beta_i = 1$ and $\eta_{ij} = 1$, two possible ground states exist and are given by $\varphi_{12} = 2\pi/3,\ \varphi_{13} = -2\pi/3$ or $\varphi_{12} = -2\pi/3,\ \varphi_{13} = 2\pi/3$. Thus in this case, the broken symmetry is $U(1) \times Z_2$, as opposed to $U(1)$. As a result, like any other system with Z_2 degeneracy, the theory al-

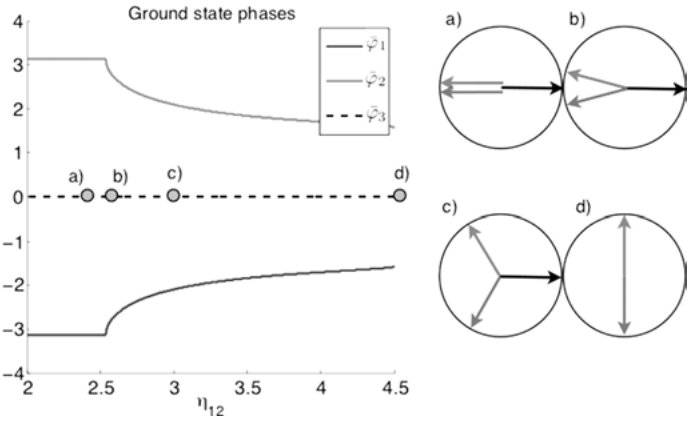

Fig. 4.5: Ground state phases of the three components as a function of η_{12} (here $\theta_3 = 0$ fixes the gauge). The GL parameters are $\alpha_i = 1$, $\beta_i = 1$, $\eta_{13} = \eta_{23} = 3$. For intermediate values of η_{12} the ground state exhibits discrete degeneracy (symmetry is $U(1) \times Z_2$ rather than $U(1)$) since the energy is invariant under the sign change $\theta_2 \to -\theta_2$, $\theta_3 \to -\theta_3$. For large η_{12} we obtain $\theta_2 - \theta_3 = \pi$ implying that $|\psi_3| = 0$ and so there is a second transition from $U(1) \times Z_2$ to $U(1)$ and only two bands at the point d). Here, the phases were computed in a system with only passive bands, though systems with active bands exhibit the same qualitative properties except for the transition to $U(1)$ and two bands only (i.e., active bands have nonzero density in the ground state).

lows an additional set of topological excitations: domain walls interpolating between the two inequivalent ground states as well as more complicated topological excitations [64–66]. Generalizations to frustrated systems with larger numbers of components was discussed in [67].

There is a divergent coherence length at the critical point where the system undergoes the $U(1) \times Z_2 \to U(1)$ phase transition (which is the transition from an $s + is$ to an s state). The nature of this divergent length-scale is revealed by calculation of the normal modes. Specifically, generating a set of differential equations from Equation (4.32) and linearizing these close to the ground state, gives a mass-matrix whose eigenbasis is also an orthonormal basis of small perturbations to the ground state [10]. In systems that break only $U(1)$ symmetry, these modes are segregated with respect to phase and amplitude so that small perturbations to the phase and amplitude sectors decay independently of each other. Small perturbations to the amplitude thus have no implications for the phase difference sector, and vice versa. In contrast, in the region where Z_2 symmetry is broken the modes are generally mixed in this kind of model. In this case a perturbation to the amplitude sector necessarily implies a perturbation to the phase sector as well and vice versa.

The immediate implication of this is that in the region with broken Z_2-symmetry, there are five rather than three coherence lengths that describe amplitude perturbations. If the phase transition is second order one of these coherence lengths diverges as we approach the transition point where Z_2-symmetry is restored. Thus, vortices in

this region produce a perturbation to the amplitude that recovers with a coherence length that is divergent. Since the magnetic field penetration depth is finite near that transition the system can be either type-1 or type-1.5 with attractive intervortex interaction [10].

In iron-based superconductors a dome of $s + is$ state is expected to form as a function of doping [9]. Away from the transition point, iron-based materials appear to be type-2. Also the amplitude of the mode with divergent coherence length vanishes at the Z_2 phase transitions. Thus, there should be a range of doping and temperatures in the proximity of the critical point where the type-1.5 superconductivity is generic. The general case of N-component frustrated superconductors is less studied, however certainly in case of a larger number of components there are more possibilities for the appearance of normal modes with low or zero masses leading to type-1.5 regimes [67].

4.8.3 Nonlinear effects and long-range intervortex interaction in $s + is$ superconductors

The ground state of a phase-frustrated superconductor is in many cases nontrivial, with phase differences being compromises between the various interaction terms. Inserting vortices in such a system can shift the balance between different competing couplings, since vortices can in general have different effects on the different bands. In particular, since the core sizes of vortices are not generally the same in all bands, vortex matter typically depletes some components more than others and thus can alter the preferred values of the phase difference. So the minimal potential energy inside a vortex lattice or cluster may correspond to a different set of phase differences than in the vortex-free ground state. In particular even in s-wave systems vortices can create "bubbles" of Z_2 order parameter around themselves. Examples are shown in Figures 4.6 and 4.7.

The vortex structure near the Z_2 phase transition has crucial physical consequences for the phase diagram of the system beyond mean-field approximation, leading to re-entrant phase transitions [68].

In the vicinity of Z_2 phase transition, besides the appearance of the type-1.5 regime, the system has a number of other unusual properties such as anomalous vortex viscosity [69] and distinct anomalous thermoelectric effects [70, 71].

4.9 Fluctuation effects in type-1.5 systems

In single-component Ginzburg–Landau models, the order of the superconducting transition in zero applied magnetic field in three dimensions depends on the ratio of magnetic field penetration length and coherence length. Halperin, Lubensky and Ma established that in extreme type-1 superconductors the gauge field fluctua-

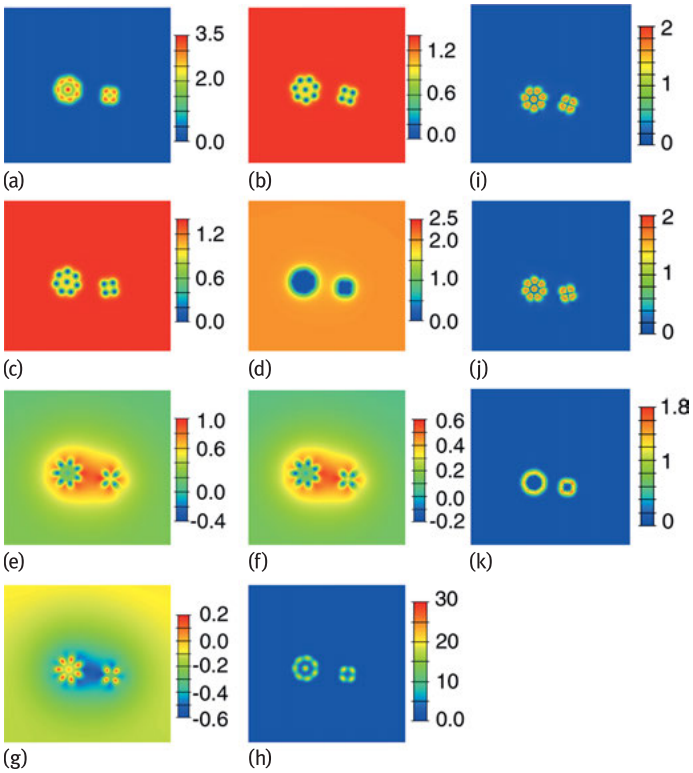

Fig. 4.6: Interacting vortex clusters with internally broken Z_2 symmetry in a frustrated three-band superconductor. The snapshot represents a slowly evolving (quasistationary) state of the weakly interacting well-separated clusters. In this numerical computation, each of the clusters has with a good accuracy converged to a physical solution of GL equations, but the snapshot is taken during the slow evolution driven by the weak long-range intercluster interaction. The snapshot demonstrates the existence of long-range field variations associated with the soft mode. This produces long-range weak intervortex forces. Displayed quantities are: (a) Magnetic field, (b–d) $|\psi_1|^2, |\psi_2|^2, |\psi_3|^2$, (e) $|\psi_1||\psi_2| \sin \varphi_{12}$, (f) $|\psi_1||\psi_3| \sin \varphi_{13}$), (g) $|\psi_1||\psi_3| \sin \varphi_{23}$). The GL parameters are $\alpha_1 = -3,\ \beta_1 = 3,\ \alpha_2 = -3,\ \beta_2 = 3, \alpha_3 = 2,\ \beta_3 = 0.5, \eta_{12} = 2.25,\ \eta_{13} = -3.7$. The parameter set was chosen so that it lies in the regime where the ground state symmetry of the system without vortices is $U(1)$, but is close to the $U(1) \times Z_2$ region. Because of the disparity in vortex core size the effective interaction strengths $\tilde{\eta}_{ij}$ are depleted to different extents. As a consequence, a vortex cluster produces a bubble of state with broken $U(1) \times Z_2$ symmetry.

tions make the superconducting phase transition first order [72, 73]. In the opposite limit of extreme type-2 systems, Dasgupta and Halperin [74] demonstrated that the superconducting transition is second order in single-component systems and has the universality class of the inverted-3DXY model. The nature of the superconducting phase transition in this limit is the proliferation of vortex-loop excitations. The inverted-3DXY universality class can be demonstrated by duality mapping [56, 74–76].

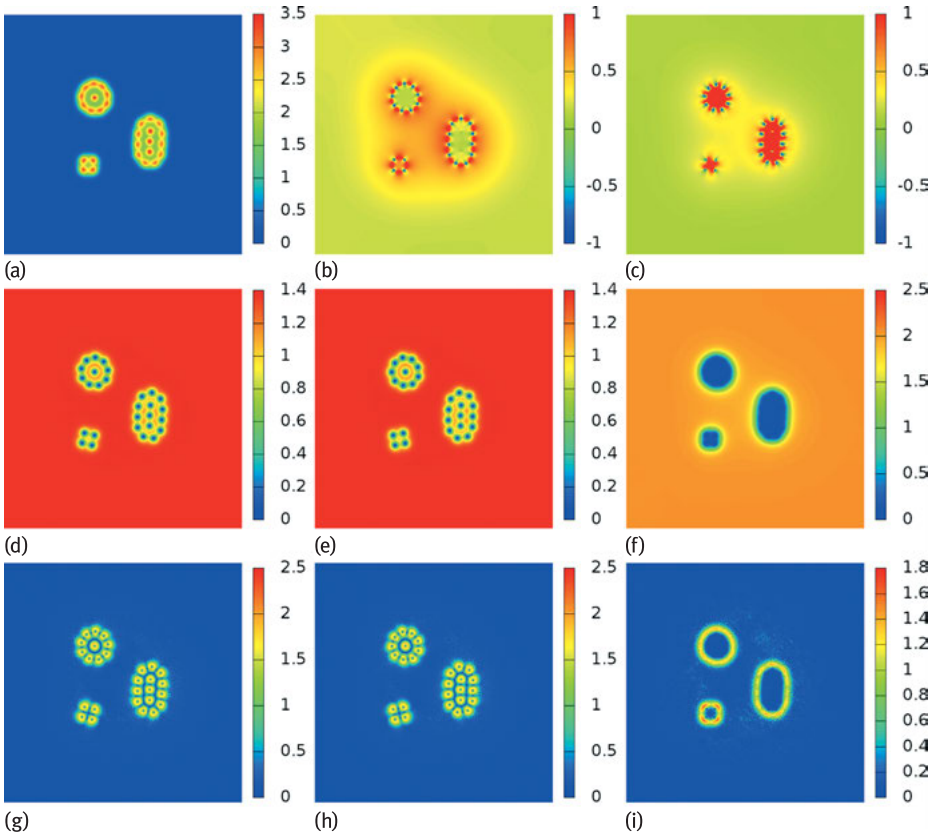

Fig. 4.7: Interacting vortex clusters with broken internal Z_2 symmetry in a frustrated three-band superconductor. Panel (a) displays the magnetic field B. Panels (b) and (c) respectively display $\sin\varphi_{12}$ and $\sin\varphi_{13}$, the third phase difference can obviously be obtained from these two. Second line, shows the densities of the different condensates $|\psi_1|^2$ (d), $|\psi_2|^2$ (e), $|\psi_3|^2$ (f). The third line displays the supercurrent densities associated with each condensate $|J_1|$ (g), $|J_2|$ (h), $|J_3|$ (i). The parameter set here is the same as in Figure 4.6. Here the difference compared to the previous picture, is that the sine of the phase differences is represented 'unweighted' by the densities in contrast to Figure 4.6, clearly indicating that vortices create an area with broken Z_2 symmetry. Panel (c) now makes clear that the inner cluster is in a defined state $\varphi_{13} \approx \pi/2$ (whose opposite state would have been $-\pi/2$). Panel (b) gives a visualization of the long-range interaction between the clusters.

The value of the Ginzburg–Landau parameter $\kappa = \lambda/\xi$ at which the phase transition changes from second to first order is difficult to establish. Early numerical works suggested that the tricritical point does not coincide with the Bogomol'nyi critical point [77]. The largest Monte Carlo simulations performed at this time [78, 79] claim that the tricritical $\kappa_{\mathrm{tri}} = (0.76 \pm 0.04)$ is slightly smaller than the critical $\kappa_{\mathrm{c}} = 1$, which, in our units, separates the type-1 regime with thermodynamically unstable vortices and the type-2 regime with thermodynamically stable vortices. In these works it

is claimed that even in the weakly type-1 regime where the vortex interaction is purely attractive and vortices are not thermodynamically stable, the phase transition can be continuous. This raises the question about the nature of the phase transition in the type-1.5 regime where by contrast vortices have long-range attractive interaction but are thermodynamically stable. The problem was investigated in the effective j-current model [80] where thermally excited vortices are modeled by directed loops with long-range attractive, short-range repulsive interaction similar to the long-range interaction between vortices in the GL model. The results indicate that the zero-field superconducting phase transition in type-1.5 materials can be first order [80]. This is in contrast to ordinary single-component GL theory which always has a continuous phase transition in the inverted 3d XY universality class in the parameter regime where vortices are thermodynamically stable. For the $s+is$ type-1.5 systems, it was found that fluctuations can modify the mean-field phase diagrams quantitatively, resulting in re-entrant phase transitions where Z_2 symmetry is broken by heating [68].

4.10 Misconceptions

In this section we clarify misconceptions about coherence lengths and type-1.5 behavior in some recent literature on one subclass of multicomponent superconductors: $U(1)$ multiband materials. An erroneous argument was advanced in [81, 82] that near T_c these superconductors have degenerate coherence lengths. Using this incorrect derivation by Kogan and Schmalian, many further papers appeared that reach various incorrect conclusions about the phase diagram and properties of these materials, for example [83–87].

Consider a two component Ginzburg–Landau model with Josephson coupling, governed by a pair of coupled partial differential equations

$$a_1\Delta_1 + b_1|\Delta_1|^2\Delta_1 - \gamma\Delta_2 - K_1\Pi^2\Delta_1 = 0 \tag{4.34}$$

$$a_2\Delta_2 + b_2|\Delta_2|^2\Delta_2 - \gamma\Delta_1 - K_2\Pi^2\Delta_2 = 0 \tag{4.35}$$

where $\Pi = \nabla - iA$. Kogan and Schmalian have argued that such a system cannot exhibit so-called type-1.5 superconductivity because close to T_c, such models inevitably have two degenerate coherence lengths in two bands, not two distinct coherence lengths as the type-1.5 regime requires. They assumed that GL functionals can only be obtained by expansion in a single small parameter $\tau = (1 - T/T_c)$. The conclusion on coherence lengths they reached by claiming that system (4.34), (4.35) is actually equivalent, for small $\tau = (1 - T/T_c)$, to the alternative system

$$-\alpha\tau\Delta_1 + \beta_1|\Delta_1|^2\Delta_1 - K\Pi^2\Delta_1 = 0 \tag{4.36}$$

$$-\alpha\tau\Delta_2 + \beta_2|\Delta_2|^2\Delta_2 - K\Pi^2\Delta_2 = 0\,. \tag{4.37}$$

Here α, β_i, K are constants that depend in a known way on the parameters a_i, b_i, K_i, γ in (4.34), (4.35). It is not hard to see that this claim is nonsensical. First of all it nei-

ther physically nor mathematically makes sense that the GL expansion can be done in only one small parameter $\tau = (1 - T/T_c)$. Multiband expansions are expansions carried in several small parameters. The limiting expression that Kogan and Schmalian obtain when $\tau \to 0$ is obviously incorrect. It suffices, for example, to note that in the absence of a gauge field, $A = 0$, system (4.36), (4.37) supports the solution with an axially symmetric vortex in Δ_1, and constant $\Delta_2 = \sqrt{\alpha\tau/\beta_2}$. Clearly, this is not a solution of (4.34), (4.35), even approximately for small τ. This is symptomatic of a fundamental problem with (4.36), (4.37): this system has no direct coupling between the condensates Δ_1, Δ_2, while such coupling is a fundamental property of (4.34), (4.35). Remarkably, Kogan and Schmalian actually state that $\Delta_1(r) = \Delta_2(r)$ but seem unaware that it directly contradicts their equations. In particular the absence of coupling between Δ_1, Δ_2, obviously directly contradicts their claim that for all solutions $\Delta_1(r) = \Delta_2(r)$, near T_c. This and other claims, such as the phase locking in [81], should follow from mathematical equations. It is not enough to simply assert behavior, particularly when the underlying model of the system contradicts one's assertions.

The claimed equivalence between (4.34), (4.35) and (4.36), (4.37) is mathematically nonsensical. It is a trivial and well-known fact that an expansion in a single small parameter $\tau = (1 - T/T_c)$ yields a single GL equation (see e.g., [18, 88, 89]). However, the authors of [81, 82] did not even recover that well-known result in the $\tau \to 0$ limit. A comment on this was written in [18, 89]. Moreover, as was pointed out in [18, 89] if taken at face value, (4.36), (4.37) imply results in direct contradiction of the Landau theory of phase transitions. In the original model (4.34), (4.35) the Josephson term is a singular perturbation that breaks symmetry down to $U(1)$. The model has three massive modes: two coherence lengths and the Josephson length. In the limit $\tau \to 0$ there can be only one divergent length scale, while the other length scales stay finite at T_c. In the $U(1)$ two-band system the gaps in the vortex solution have a similar profile near T_c or at strong coupling because there is a subdominant with much shorter coherence length and small amplitude that is associated with a certain linear combination of the fields. This can be demonstrated by explicit calculation [18, 23, 89] and this is the reason why similar gap profiles should be observed in experiment on such systems [87]. In contrast, Kogan and Schmalian's system gives the opposite behavior: three independently divergent length scales in the limit $\tau \to 0$, since (4.36), (4.37) are coupled by the vector potential only, the mass of the Leggett mode also would vanish.

It is interesting to follow Kogan and Schmalian's derivation of (4.36), (4.37), to identify exactly where the error occurs. They first solve (4.34) to find Δ_2 in terms of Δ_1 and its derivatives

$$\Delta_2 = \frac{1}{\gamma}\left(a_1\Delta_1 + b_1|\Delta_1|^2\Delta_1 - K_1\Pi^2\Delta_1\right) \tag{4.38}$$

then use this to eliminate Δ_2 from (4.35), yielding a fourth-order PDE for Δ_1 alone,

$$a_1'\Delta_1 + b_1'|\Delta_1|^2\Delta_1 + \cdots + K_1'\Pi^4\Delta_1 = 0 \tag{4.39}$$

whose coefficients, $a_1', b_1', \ldots, K_1'$ depend in a known way on a_i, b_i, K_i, γ. Of course, system (4.38), (4.39) is exactly equivalent to (4.34), (4.35). They then note that indeed the same procedure works with the roles of Δ_1 and Δ_2 reversed: solve (4.35) for Δ_1 in terms of Δ_2, and eliminate Δ_1 from (4.34). This yields the system

$$\Delta_1 = \frac{1}{\gamma}\left(a_2\Delta_2 + b_2|\Delta_2|^2\Delta_2 - K_2\Pi^2\Delta_2\right) \tag{4.40}$$

$$a_2'\Delta_2 + b_2'|\Delta_2|^2\Delta_2 + \cdots + K_2'\Pi^4\Delta_2 = 0 \tag{4.41}$$

which, like (4.38), (4.39), is equivalent to (4.34), (4.35). They then perform two procedures. First they truncate (4.39) and (4.41) to second order, by making assumptions about which terms dominate at small τ. This yields equations (4.36) and (4.37). If executed properly the assumption of one small parameter should yield a single GL equation and one cannot deduce any information about the second mode and second coherence length. Second, and more important, they completely forget about the equations (4.38), (4.40), as though these relations no longer hold. What results is a system of equations, (4.36), (4.37), which have *absolutely no relationship* with the original system (4.34), (4.35).

In summary, system (4.36), (4.37) tells us precisely nothing about the behavior of the solutions of (4.34), (4.35) or behavior of two coherence lengths or relative behavior of the gaps near T_c.

The paper [84], develops an elaboration of (4.36), (4.37), in which the fields Δ_j are claimed to be expanded in a power series in $\tau = 1 - T/T_c$

$$\Delta_j = \Delta_j^{(0)} + \Delta_j^{(1)} + \cdots \tag{4.42}$$

where $\Delta_j^{(0)}$ is the term of order $\tau^{\frac{1}{2}}$ and $\Delta_j^{(1)}$ is the term of order $\tau^{\frac{3}{2}}$ (note that the results are inconsistent by symmetry in different order in τ and also the two-band GL expansion is not a τ-based expansion and cannot be carried in a single small parameter in general). Since the procedure is based on Kogan and Schmalian's construction, the above criticism applies equally to these works. Although the analysis is incorrect for multiband superconductors, as shown above, let us take their final system of equations at face value and analyze it purely from a mathematical viewpoint.

The system obtained is (they consider only the case where there is no gauge field and absorb K into a choice of units).

$$-\nabla^2\Delta_j^{(0)} + \alpha\Delta_j^{(0)} + \beta_j{\Delta_j^{(0)}}^3 = 0\,, \tag{4.43}$$

$$-\nabla^2\Delta_j^{(1)} + (\alpha + 3\beta_j{\Delta_j^{(0)}}^2)\Delta_j^{(1)} = f_j \tag{4.44}$$

where f_j is a polynomial expression in $\Delta_j^{(0)}$ and its derivatives (up to fourth order). The first thing to note is that this is *not* a fourth-order system of PDEs: $\Delta_j^{(0)}$ is already fixed by solving a second-order PDE (4.43), and given this, one solves another *second-order* PDE for $\Delta_j^{(1)}$. The second thing to note is that (4.44) can be economically and

instructively written

$$L_j \Delta_j^{(1)} = f_j \tag{4.45}$$

where L_j is the (formally) self-adjoint linear operator obtained by linearizing (4.43) about its solution $\Delta_j^{(0)}$. Now, a linear PDE of this form will have a solution if and only if f_j is L^2 orthogonal to the kernel of the operator L_j, that is,

$$\int_{\mathbb{R}^3} f_j k d^3x = 0 \quad \text{for all } k \text{ such that } L_j k = 0 \,. \tag{4.46}$$

While this condition holds automatically if the kernel is trivial (the only solution of $L_j k = 0$ is $k = 0$), in the current context, this is highly unlikely, as we now argue.

Given a solution $\Delta_j^{(0)}$ of (4.43), one would expect it to lie in a finite dimensional family of solutions, obtained, for example, by translating and rotating the given solution. But for every one-parameter family of solutions $\Delta_j^{(0)}(t)$ of (4.43), there is a function in the kernel of L_j, namely

$$k = \partial_t \Delta_j^{(0)}(t)|_{t=0} \,. \tag{4.47}$$

To see this, just substitute $\Delta_j^{(0)}(t)$ into (4.43) and differentiate with respect to the parameter t, using the fact that each $\Delta_j^{(0)}(t)$ solves (4.43).

Hence, generically the right hand side f_j of (4.44) must satisfy a large number of nontrivial integral constraints, or else the system has no solution. Furthermore, if f_j *does* satisfy the constraints, the solution $\Delta_j^{(1)}$ is generically not unique, since one can add to it any k in the kernel of L_j.

It should also be emphasized that, since (4.43), (4.44) is derived from (4.36), (4.37), it, also, has no mathematical relationship to the original system (4.34), (4.35) nor with the microscopic theory of two-band superconductors. It is also physically meaningless in general to justify two-band field theories by expansion in a single small parameter τ. Also, in contrast to false claims in [83] it contradicts other standard schemes of Ginzburg–Landau expansion in systems with different pairing channels [90] and basic symmetry-based aspects of the theory of second-order phase transitions. The conclusion of independent divergence of coherence lengths, that contradicts basic principles of the theory of the phase transitions, leads to the construction of incorrect phase diagrams in [86], and the erroneous claim that there necessarily appears a Bogomol'nyi point near T_c. The necessary condition for a Bogomol'nyi point in this kind of theory is to generate masses of the normal modes. As discussed above the degenerate coherence length is a direct consequence of the mathematical error in Kogan and Schmalian's calculations. In real two-band superconductors, the masses of normal modes as functions of interband coupling or temperature never cross but rather form avoided crossing [18, 23, 89], unless there is a special symmetry of the model.

4.11 Conclusion

We briefly outlined the basic concepts and gave a brief account of some of the works on type-1.5 superconductivity that takes place in multicomponent systems. In general, a superconducting state is characterized by multiple coherence lengths ξ_i, ($i = 1, \ldots, M$) arising from multiple broken symmetries or multiple bands. The type-1.5 state is the regime where some of the coherence lengths are larger and some smaller than the magnetic field penetration length: $\xi_1 \leq \xi_2 \ldots < \lambda < \xi_N \leq \ldots \leq \xi_N$ (here we absorbed the factor $1/\sqrt{2}$ into the definition of coherence lengths). Among various unconventional properties that the system acquires in this regime is nonmonotonic intervortex interaction potential. In that state vortices can have long-range attractive, short-range repulsive interaction leading to a macroscopic phase separation into domains of Meissner and vortex states in an applied external field. This phase separation can also be accompanied by different broken symmetries in vortex clusters and Meissner domains. This regime leads to unconventional magnetic, thermal and transport properties.

Acknowledgment: We thank Julien Garaud for discussions and collaboration on this project. The work was supported by the Swedish Research Council Grant. No. 642-2013-7837 and Goran Gustafsson Foundation. J.C. was supported by the Wenner-Gren Foundation. The computations were performed on resources provided by the Swedish National Infrastructure for Computing (SNIC) at the National Supercomputer Center at Linköping, Sweden.

Bibliography

[1] Landau L, Ginzburg V. Zh. Eksp. Teor. Fiz 20:546, 1950.
[2] De Gennes P. Superconductivity of Metals and Alloys (Advanced Book Classics). Addison-Wesley Publ. Company Inc, 1999.
[3] Abrikosov AA. Sov. Phys.-JETP (Engl. Transl.); (United States) 5:1174–1182, 1957.
[4] Kramer L. Phys. Rev. B 3:3821, 1971.
[5] Bogomol'nyi E. Sov. J. Nucl. Phys. (Engl. Transl.); (United States) 24:4, 1976.
[6] Jacobs A. J. Low Temp. Phys. 10:137, 1973.
[7] Carlström J, Babaev E, Speight M. Phys. Rev. B 83:174509, 2011.
[8] Stanev V, Tešanović Z. Phys. Rev. B 81:134522, 2010.
[9] Maiti S, Chubukov AV. Phys. Rev. B 87:144511, 2013.
[10] Carlström J, Garaud J, Babaev E. Phys. Rev. B 84:134518, 2011.
[11] Babaev E, Sudbø A, Ashcroft N. Nature 431:666, 2004.
[12] Herland EV, Babaev E, Sudbø A. Physical Review B 82:134511, 2010.
[13] Jones PB. Monthly Notices of the Royal Astronomical Society 371:1327, 2006, http://arxiv.org/abs/http://mnras.oxfordjournals.org/content/371/3/1327.full.pdf+html.
[14] Babaev E. Physical review letters 103:231101, 2009.
[15] Suhl H, Matthias BT, Walker LR. Phys. Rev. Lett. 3:552, 1959.

[16] Leggett AJ. Progress of Theoretical Physics 36:901, 1966.
[17] Tilley D. Proceedings of the Physical Society 84:573, 1964.
[18] Silaev M, Babaev E. Phys. Rev. B 85:134514, 2012.
[19] Frank RL, Lemm M. Annales Henri Poincaré, 1:2285–2340, 2016.
[20] Garaud J, Agterberg DF, Babaev E. Phys. Rev. B 86:060513, 2012.
[21] Babaev E, Speight M. Phys. Rev. B 72:180502, 2005.
[22] Babaev E, Carlström J, Speight M. Phys. Rev. Lett. 105:067003, 2010.
[23] Silaev M, Babaev E. Phys. Rev. B 84:094515, 2011.
[24] Carlström J, Garaud J, Babaev E. Phys. Rev. B 84:134515, 2011.
[25] Moshchalkov V, Menghini M, Nishio T, Chen QH, Silhanek AV, Dao VH, Chibotaru LF, Zhigadlo ND, Karpinski J. Phys. Rev. Lett. 102:117001, 2009.
[26] Nishio T, Dao VH, Chen Q, Chibotaru LF, Kadowaki K, Moshchalkov VV. Phys. Rev. B 81:020506, 2010.
[27] Hicks CW, Kirtley JR, Lippman TM, Koshnick NC, Huber ME, Maeno Y, Yuhasz WM, Maple MB, Moler KA. Phys. Rev. B 81:214501, 2010.
[28] Ray SJ, Gibbs AS, Bending SJ, Curran PJ, Babaev E, Baines C, Mackenzie AP, Lee SL. Phys. Rev. B 89:094504, 2014.
[29] Kawasaki I, Watanabe I, Amitsuka H, Kunimori K, Tanida H, Ōnuki Y. J. Phys. Soc. Jpn. 82:084713, 2013.
[30] Fujisawa T, Yamaguchi A, Motoyama G, Kawakatsu D, Sumiyama A, Takeuchi T, Settai R, Ånuki Y. Jpn. J. Appl. Phys. 54:048001, 2015.
[31] Agterberg DF, Babaev E, Garaud J. Phys. Rev. B 90:064509, 2014.
[32] Parameswaran S, Kivelson S, Rezayi E, Simon S, Sondhi S, Spivak B. Physical Review B 85:241307, 2012.
[33] Alford MG, Good G. Physical Review B 78:024510, 2008.
[34] Dao VH, Chibotaru LF, Nishio T, Moshchalkov VV. Phys. Rev. B 83:020503, 2011.
[35] Geurts R, Milošević M, Peeters F. Phys. Rev. B 81:214514, 2010.
[36] Gutierrez J, Raes B, Silhanek A, Li L, Zhigadlo N, Karpinski J, Tempere J, Moshchalkov V. Phys. Rev. B 85:094511, 2012.
[37] Li L, Nishio T, Xu Z, Moshchalkov V. Phys. Rev. B 83:224522, 2011.
[38] Varney CN, Sellin KA, Wang Q-Z, Fangohr H, Babaev E. J. Phys.: Condens. Matter 25:415702, 2013.
[39] Wang J-P. Phys. Rev. B 82:132505, 2010.
[40] Drocco JA, Reichhardt CJO, Reichhardt C, Bishop AR. J. Phys.: Condens. Matter 25:345703, 2013.
[41] Meng Q, Varney CN, Fangohr H, Babaev E. Phys. Rev. B 90:020509, 2014.
[42] Garaud J, Babaev E. Phys. Rev. B 91:014510, 2015.
[43] Edström A. Physica C: Superconductivity 487:19, 2013.
[44] Gurevich A. Phys. Rev. B 67:184515, cond-mat/0212129, 2003.
[45] Gurevich A. Physica C: Superconductivity 456:160, 2007.
[46] Zhitomirsky ME, Dao V-H. Phys. Rev. B 69:054508, 2004.
[47] Garaud J, Silaev M, Babaev E. Physica C 533:63–73, 2017.
[48] Babaev E. Phys. Rev. Lett. 89:067001, 2002.
[49] Babaev E, Speight JM. Phys. Rev. B 72:180502, 2005.
[50] Speight JM. Phys. Rev. D 55:3830, hep-th/9603155, 1997.
[51] Manton NS, Sutcliffe P. Topological solitons. Cambridge, UK: Cambridge University Press, 2004.
[52] Pearl J. Appl. Phys. Lett. 5:65, 1964.

[53] Bogomol'nyi E, Vainshtein A. Sov. J. Nucl. Phys. (Engl. Transl.); (United States) 23:588–591, 1976.
[54] Saint-James D, Sarma G, Thomas EJ. TYPE-II SUPERCONDUCTIVITY., Tech. Rep. CEN, Saclay, France, 1969.
[55] Shifman M. Advanced Topics in Quantum Field Theory: A Lecture Course. Cambridge University Press, 2012.
[56] Svistunov BV, Babaev ES, Prokof'ev NV. Superfluid states of matter. Crc Press, 2015.
[57] Leung MC, Jacobs AE. J. Low Temp. Phys. 11:395, 1973.
[58] Eilenberger G, Büttner H. Z. Phys. 224:335, 1969.
[59] Meng Q, Varney CN, Fangohr H, Babaev E. J. Phys.: Condens. Matter 29:035602, 2017
[60] Diaz-Mendez R, Mezzacapo F, Lechner W, Cinti F, Babaev E, Pupillo G. Phys. Rev. Lett. 118:067001, 2017.
[61] Smørgrav E, Smiseth J, Babaev E, Sudbø A. Physical review letters 94:96401, 2005.
[62] Ng TK, Nagaosa N. Europhysics Letters 87:17003, 2009.
[63] Lin S-Z, Hu X. Phys. Rev. Lett. 108:177005, 2012.
[64] Garaud J, Carlström J, Babaev E. Phys. Rev. Lett. 107:197001, 2011.
[65] Garaud J, Carlström J, Babaev E, Speight M. Phys. Rev. B 87:014507, 2013.
[66] Garaud J, Babaev E. Phys. Rev. Lett. 112:017003, 2014.
[67] Weston D, Babaev E. Phys. Rev. B 88:214507, 2013.
[68] Carlström J, Babaev E. Phys. Rev. B 91:140504, 2015.
[69] Silaev M, Babaev E. Phys. Rev. B 88:220504, 2013.
[70] Silaev M, Garaud J, Babaev E. Phys. Rev. B 92:174510, 2015.
[71] Garaud J, Silaev M, Babaev E. Physical Review Letters 116:097002, arXiv:1507.04712 [cond-mat.supr-con], 2016.
[72] Halperin BI, Lubensky TC, Ma S-K. Phys. Rev. Lett. 32:292, 1974.
[73] Coleman S, Weinberg E. Phys. Rev. D 7:1888, 1973.
[74] Dasgupta C, Halperin BI. Phys. Rev. Lett. 47:1556, 1981.
[75] Peskin ME. Annals of Physics 113:122, 1978.
[76] Thomas PR, Stone M. Nuclear Physics B 144:513, 1978.
[77] Bartholomew J. Phys. Rev. B 28:5378, 1983.
[78] Mo S, Hove J, Sudbø A. Phys. Rev. B 65:104501, 2002.
[79] Hove J, Mo S, Sudbø A. Phys. Rev. B 66:064524, 2002.
[80] Meier H, Babaev E, Wallin M. Phys. Rev. B 91:094508, 2015.
[81] Kogan VG, Schmalian J. Phys. Rev. B 83:054515, 2011.
[82] Kogan VG, Schmalian J. Phys. Rev. B 86:016502, 2012.
[83] Orlova NV, Shanenko AA, Milošević MV, Peeters FM, Vagov AV, Axt VM. Phys. Rev. B 87:134510, 2013.
[84] Shanenko AA, Milošević MV, Peeters FM, Vagov AV. Phys. Rev. Lett. 106:047005, 2011.
[85] Vagov AV, Shanenko AA, Milošević MV, Axt VM, Peeters FM. Phys. Rev. B 85:014502, 2012.
[86] Vagov A, Shanenko A, Milošević M, Axt V, Vinokur V, Peeters F. Arxiv preprint, arXiv:1311.5624, 2013.
[87] Fente A, Herrera E, Guillamón I, Suderow H, Mañas Valero S, Galbiati M, Coronado E, Kogan VG. Phys. Rev. B 94:014517, 2016.
[88] Geilikman B, Zaitsev R, Kresin V. Sov. Phys.-Solid State (Engl. Transl.) 9:642–651, 1967.
[89] Babaev E, Silaev M. Phys. Rev. B 86:016501, 2012; arXiv:1105.3756.
[90] Sigrist M, Ueda K. Rev. Mod. Phys. 63:239, 1991.